Heliyon 12 (2026) e45086

Contents lists available at ScienceDirect

Heliyon

journal homepage: www.cell.com/heliyon

Research article

# Vegetation recovery amid conflicts: Analysis of land use land cover changes in Darfur, Sudan, using high-resolution satellite imagery

Abdalrahman Ahmed [a,b,*], Brian Rotich [c], Harison Kiplagat Kipkulei [d], Kornel Czimber [a]

[a] *Institute of Geomatics and Civil Engineering, Faculty of Forestry, University of Sopron. Bajcsy-Zs 4, Sopron, 9400, Hungary*
[b] *Department of Forest and Environment, Faculty of Forest Sciences and Technology, University of Gezira, P.O. Box 20, Wad Madani, Sudan*
[c] *Faculty of Environmental Studies and Resources Development, Chuka University, P.O. Box 109-60400, Chuka, Kenya*
[d] *Department of Geomatic Engineering and Geospatial Information Systems, Jomo Kenyatta University of Agriculture and Technology, P.O. Box, 62000 00200, Nairobi, Kenya*

ARTICLE INFO

*Keywords:*
Conflicts
IDPs
PlanetScope
Support vector machine
Reforestation
Ecological recovery

ABSTRACT

The prolonged conflict in Sudan's Darfur region has led to extensive displacement of local populations. This study uses advanced high-resolution satellite imagery to explore the complex effects of long-term conflicts on land use management in Darfur, Sudan. It highlights positive changes in vegetation cover near internally displaced persons (IDPs) camps and examines land use and land cover (LULC) change trends from 2017, 2019, 2021, and 2023. Utilizing PlanetScope time-series imagery and Object-based Image Analysis (OBIA) with Orfeo ToolBox 8.1.2 in QGIS 3.28.6. and the Standardized Precipitation-Evapotranspiration Index (SPEI), we assessed vegetation dynamics in relation to drought conditions in the study region. The research identified six major LULC classes including agricultural land, bareland, water bodies, vegetation cover, built-up areas, and wadi through supervised classification, achieving an overall accuracy ranging from 90.66% to 95.14%. The findings reveal a significant increase in vegetation cover from 182.76ha (0.75%) in the year 2017 to 391.09ha (1.60%) in 2023, marking a 208.33ha (113.99%) expansion over the study period. Water bodies also increased from 0.18ha (0.001%) in 2017 to 3.34ha in 2023 (0.014%). These improvements are attributed to annual reforestation efforts by the Forest National Corporation (FNC), the construction of artificial water harvesting aquifers, and a general increase in mean annual rainfall from 2014 to 2022 aligning with reduced drought intensity in the study area. Additionally, bareland areas decreased rapidly from 46.82% to 39.31%, while agricultural land expanded from 48.26% to 54.61% between 2017 and 2023. This research provides valuable insights into the positive environmental impacts of afforestation and reforestation efforts in conflict-affected regions. The results emphasize the critical role of IDPs in supporting the global sustainable development agenda, particularly in the restoration and conservation of terrestrial ecosystems within conflict-affected zones. Moreover, the study demonstrates the potential for substantial ecological recovery in the study area.

* Corresponding author. Institute of Geomatics and Civil Engineering, Faculty of Forestry, University of Sopron. Bajcsy-Zs 4, Sopron, 9400, Hungary

*E-mail address:* ix3mzk@uni-sopron.hu (A. Ahmed).

https://doi.org/10.1016/j.heliyon.2026.e45086
Received 23 September 2024; Received in revised form 3 June 2026; Accepted 4 June 2026
Available online 10 June 2026

## 1. Introduction

Over the past century, environmental degradation and land use change have become major global concerns, particularly in arid and semi-arid regions where natural resources are limited and ecosystems are highly vulnerable to disturbance [1]. Land use and land cover (LULC) changes can significantly affect biodiversity, ecosystem services, soil productivity, and water resources, thereby influencing the livelihoods and well-being of local communities [2,3]. In regions experiencing large-scale population displacement, changes in land use patterns may increase pressure on natural resources; however, under certain conditions, environmental restoration initiatives, sustainable land management practices, and community participation can also contribute to positive ecological outcomes, including vegetation recovery and landscape rehabilitation. For example, in Ethiopia, IDPs have participated in reforestation and land rehabilitation projects, such as planting trees and restoring degraded lands, which help combat desertification and improve local ecosystems [4] Similarly, in Kenya, refugee communities have engaged in agroforestry, integrating trees and shrubs into agricultural landscapes, thereby enhancing biodiversity and soil health [5]. IDPs often bring traditional knowledge and sustainable agricultural practices to their new locations, leading to the adoption of environmentally friendly farming techniques, such as crop rotation and organic farming, which enhance soil health and biodiversity [6].

Climate change has become a pressing global challenge, drawing increasing attention from scientists, policymakers, and the general public due to its profound effects on ecosystems, agriculture, water resources, energy supplies, and human health [7,8]. Variability in temperature and precipitation has exerted both positive and negative impacts on ecosystems, particularly in developing countries where climate-induced changes exacerbate existing environmental and socio-economic vulnerabilities [9,10].

In Africa, the impacts of climate change are expected to intensify existing vulnerabilities, with many regions already experiencing extreme temperatures, low precipitation, frequent droughts, food insecurity, and water scarcity. The Intergovernmental Panel on Climate Change (IPCC) projects that temperature increases in the Sahel region will exceed the global average, leading to more frequent heatwaves, prolonged dry spells, and heightened desertification risks [11,12]. Sudan, located within this ecologically sensitive zone, is particularly vulnerable to climate variability, with multiple compounding factors such as endemic poverty, weak institutions, limited access to capital, environmental degradation, and conflict further exacerbating climate-related challenges [13]. Despite these challenges, recent studies indicate that shifts in precipitation patterns, alongside targeted land management strategies, can facilitate vegetation recovery in degraded landscapes [14,15]. Understanding the interplay between climate variability, land use changes, and ecological restoration is crucial for sustainable development, particularly in areas affected by displacement and resource pressures.

Afforestation and reforestation have been practiced in Sudan since 1911, with significant acceleration following the establishment of the Forest National Corporation (FNC) in 1989. Internationally funded projects such as those by the Food and Agricultural Organization (FAO), United Nations Development Program (UNDP), and International Fund for Agricultural Development (IFAD), alongside community initiatives, have contributed to forest rehabilitation [16]. These efforts depend on consistent financial resources from national and international source [17,18]. Notably, refugee-driven projects in South Darfur, Gadarif, Kassala, and White Nile states focus on restoring degraded lands and promoting energy alternatives, including improved stoves and solar energy [19]. Although research on agroforestry and forest rehabilitation in Sudan is still developing, some studies provide insights into the impacts of tree cropping systems on livelihoods and environmental recovery [20]. The 2015 National Biodiversity Strategy (NBS) emphasizes biodiversity conservation and community participation in forest management [21].

Drought is a major environmental challenge affecting arid and semi-arid regions, including Sudan, where prolonged dry conditions have significant implications for ecosystems, agriculture, and human livelihoods [22]. With the increasing global temperatures, drought frequency and intensity are projected to rise, exacerbating environmental degradation and resource scarcity. Traditionally, drought assessment has relied on precipitation-based indices such as the Standardized Precipitation Index (SPI). However, SPI does not account for temperature effects, which are crucial in driving drought severity under global warming [23,24]. To address this limitation, the Standardized Precipitation Evapotranspiration Index (SPEI) was developed. Unlike SPI, SPEI integrates temperature and potential evapotranspiration (PET), providing a more comprehensive measure of drought severity [25]. Given Sudan's high temperature variability, SPEI was selected as the primary drought index for this study. Additionally, advancements in LULC classification have introduced various methodologies to improve accuracy. While Maximum Likelihood Classification (MLC) remains widely used, nonparametric techniques such as Support Vector Machines (SVMs), Decision Trees (DT), and Artificial Neural Networks (ANNs) have demonstrated higher accuracy in LULC extraction [26,27]. More recently, deep learning-based classification methods, including Convolutional Neural Networks (CNNs) and TensorFlow frameworks have been employed in remote sensing applications. However, these models require extensive labelled training datasets, which are often challenging to obtain. Given these considerations, our study integrates NDVI-based classification to enhance classification reliability.

Remote sensing has proven valuable for assessing the impact of human activity on ecosystems, particularly in conflict zones, where it helps track environmental degradation, vegetation health, and recovery rates [28]. It has also been employed to monitor war-related damage and conflict events, including the displacement of populations [29]. Recent studies have used remote sensing to track land use/land cover (LULC) changes due to armed conflict in Darfur using machine learning [30]. Although these studies have attempted to evaluate the link between conflicts and land use changes, there is still more that needs to be done to examine the role of restoration activities, especially the impact brought by displaced persons in addressing the negative effects of land use transformations. This study provides a novel perspective on vegetation recovery in the context of IDPs camps by integrating high-resolution satellite-based LULC classification with an analysis of climate variability. Unlike previous studies, which primarily focus on the socio-economic impacts of displacement, our research emphasizes the environmental implications of IDP settlements and their role in landscape transformation. Therefore, this study aims to: (1) Assess changes in vegetation cover around the El-Salam IDP camp using high-resolution satellite imagery. (2) Analyze the role of climate variability, particularly precipitation and drought intensity, as key drivers of vegetation recovery. (3) Evaluate the impact of reforestation activities on environmental recovery, aligning with Sustainable Development Goal (SDG) 15 (Life on Land). By addressing these objectives, our research contributes to the growing body of knowledge on sustainable land management in conflict-affected regions, offering insights that can inform policy and climate adaptation strategies.

## 2. Methods

### *2.1. Study area*

El-Salam IDP camp is located in South Darfur, Sudan, between 11°53′ and 12°0′ North and 24°51′ and 25°4′ East (Fig. 1(a–c)). The research area covers approximately 24,437.35 ha. Established in 2004, the camp has experienced significant population dynamics, with the IDP population reaching 57,806 as of 2017 [31]. The camp is situated near a wadi, where the majority of the IDPs engage in agriculture (rain-fed and irrigated) during the rainy season from June to September. Originally a small village named Hashaba before the Darfur conflict, the camp has grown to include nearly square compounds bounded by walls or fences and separated by narrow roads. Dwellings in the camp range from traditional huts to tents, with brighter dwellings and corrugated-iron structures for marketplaces, schools, and clinics. The area contains various LULC types, including water bodies, agricultural land, bareland, Wadi sand, and vegetation.

### *2.2. The flora*

Sandy Soil Vegetation: The dominant species in the study area are *Acacia senegal*, valued for its production of Gum Arabic, and *Leptadenia pyrotechnica*, a rapidly growing desert tree.

Clay Soil Vegetation: Dominant species include *Acacia mellifera, Boscia senegalensis, Capparis decidua*, and *Balanites aegyptiaca*. These species were significantly degraded at the onset of the IDPs' arrival but have been rehabilitated in recent years. During this time, the majority of species in the Wadis provided benefits such as grazing, shelter, recreation, and firewood collection to the IDP communities (field observation 2021).

Agroforestry: Trees in this habitat, including *Ziziphus spina-christi, Khaya senegalensis*, and *Eucalyptus spp*, have been largely cultivated alongside crops as part of agroforestry practices.

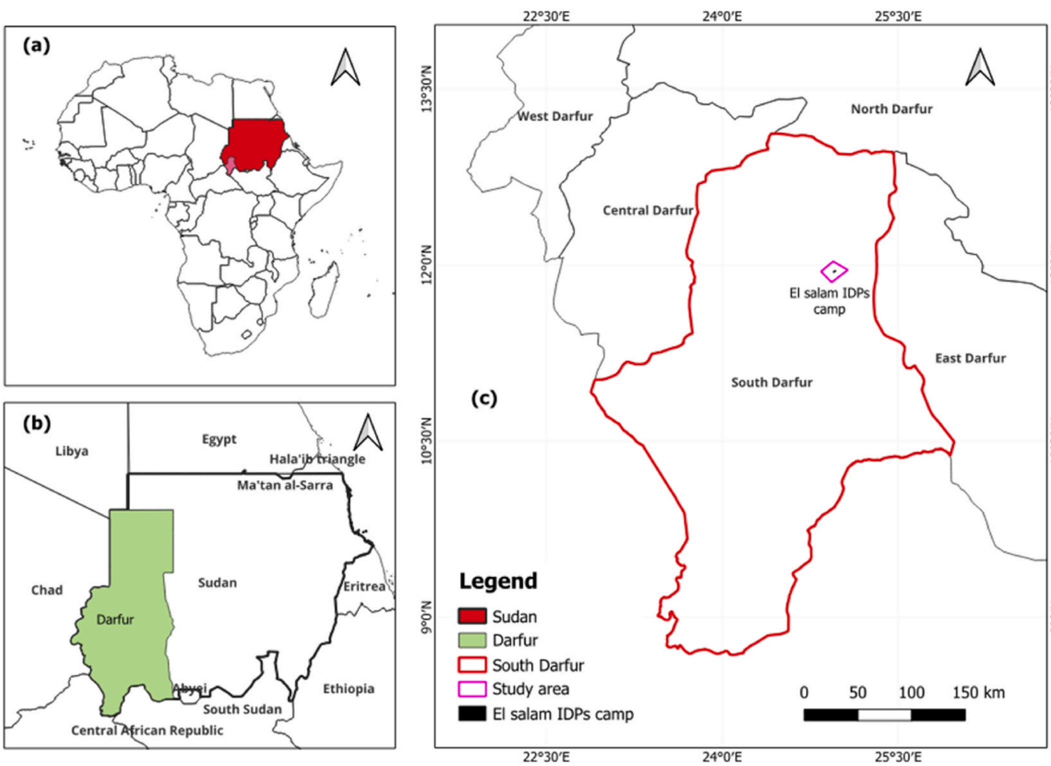


**Fig. 1.** Map of the study area showing (a) Location of Sudan in Africa (b) Location of Darfur region in Sudan (c) Location of the study area in South Darfur.

### 2.3. Satellite data

Multispectral, cloud-free images from the PlanetScope mission (https://www.planet.com/) were utilized as the primary data source for this study, covering the years 2017, 2019, 2021, and 2023. These observations began three years after the launch of the afforestation program in 2014. The images, consisting of four spectral bands (red, green, blue, and infrared), with a spatial resolution of 3.5 m enabled precise monitoring of land cover changes and vegetation dynamics, which were critical for assessing the success of the reforestation and land management initiatives implemented in the region (Table 1). The PlanetScope mission, comprising over 350 active nano satellites, is capable of imaging the Earth's entire landmass daily. The images were provided free of charge for scientific purposes, as mentioned in the acknowledgments section. All data were projected to the Universal Transverse Mercator (UTM) projection system, zone 35N, with the World Geodetic System 84 (WGS84) datum, ensuring consistency across datasets during analysis. Preprocessing was performed using QGIS 3.28.6 software. In this study, all satellite imagery was acquired during the dry season (January) to minimize the impact of seasonal variability on LULC classification. Selecting imagery from a consistent season across different years ensures comparability and reduces discrepancies caused by temporary vegetation changes during the rainy season. To further address potential seasonal variations, we incorporated vegetation indices such as the Normalized Difference Vegetation Index (NDVI) to distinguish between seasonal greening and long-term vegetation changes. This approach helps ensure that observed trends reflect permanent land cover transformations rather than short-term fluctuations. Our methodology aligns with previous studies, such as [32], which highlights the importance of using dry-season imagery for LULC classification in semi-arid regions to enhance accuracy and comparability.

### 2.4. Reference data

The collection of ground truth data is a major constraint for such conflict areas, especially in the level of detail. Therefore, a visual interpretation based on the satellite images of the IDP camp was conducted to distinguish between the different LULC classes. The NDVI threshold for the separation of vegetation and the historical high-resolution images on the Google Earth platform were used as reference data to increase the classification accuracy. Being aware that visual interpretation is also subject to errors, it was the only possibility to get comparative figures for the study area.

### 2.5. Image segmentation and classification

Image segmentation is an important step in object-based image analysis (OBIA). OBIA is becoming an increasingly important technology for information extraction from remote sensing images [33]. We used the Meanshift segmentation algorithm available in QGIS 3.28.6, known as OrfeoToolBox (OTB). The Mean Shift Segmentation algorithm was chosen for this study due to its non-parametric, density-based clustering approach, which effectively delineates homogeneous land cover regions without requiring prior assumptions about the number of segments [34]. Unlike other segmentation techniques such as k-means clustering or watershed segmentation, Mean Shift offers several advantages: Preserves spatial continuity by grouping pixels with similar spectral and spatial properties, minimizing noise and fragmentation in the classification process. It is also less sensitive to parameter tuning than edge-detection or region-growing algorithms, making it more adaptable to complex landscapes. Performs well with high-resolution imagery, which is crucial for accurately mapping vegetation and land use changes in heterogeneous environments. Mitigates over-segmentation, a common issue with other methods, by adaptively merging regions based on spectral similarity.

Before image classification, we used the raster calculator tool in QGIS to calculate NDVI using equation (1). This commonly used method describes the discrepancy between the amount of near-infrared and red light reflected by vegetation. Photosynthesizing vegetation absorbs red light and reflects near-infrared light, resulting in areas with healthy vegetation having NDVI values close to 1. On the other hand, areas with reduced photosynthetic activity absorb proportionally less visible light reflect less near-infrared light, and so have lower NDVI value. For the same reason, bare ground tends to reflect red and near-infrared light evenly and so has NDVI values close to 0. Water has negative NDVI values because it absorbs near-infrared much more than red light

$$NDVI = \frac{NIR - Red}{NIR + Red} \qquad \text{Equation (1)}$$

Then supervised LULC classification was conducted based on manually collected training samples for six predefined classes: agricultural land, bareland, water bodies, vegetation cover, built-up areas, and Wadi (Table 2). Training samples were strategically selected across diverse LULC types to ensure a comprehensive representation of the study area, following best practices outlined by Ref. [35]. A minimum of 120 samples per class was randomly collected, using a stratified random sampling approach to maintain an

**Table 1**
Summary of images utilized in this study.

| Acquisition Date | Data Source | Resolution (m) | Bands | Parameter of Interest |
|---|---|---|---|---|
| 2017-01-14 | PlanetScope Scene | 3.5 | RGB + NIR | Land use/Land cover |
| 2019-01-07 | PlanetScope Scene | 3.5 | RGB + NIR | Land use/Land cover |
| 2021-01-11 | PlanetScope Scene | 3.5 | RGB + NIR | Land use/Land cover |
| 2023-01-16 | PlanetScope Scene | 3.5 | RGB + NIR | Land use/Land cover |

**Table 2**
Description of the LULC classification scheme used for this study.

| LULC class | Description |
|---|---|
| Agricultural land | Dry farmland (rain-fed/irrigated) used to cultivate cereal crops, maize, sorghum, legumes (beans). It also includes farmlands mixed with agroforestry trees mainly *Eucaliptus spp*, *valdherbia albida*, *khaya senegalensis*, *ziziphus spina-crirty* and fruit gardens like lemon, orange, and mango. |
| Bareland | Include areas dominated by barren rock, eroded, and degraded lands, and other soil surfaces that remain devoid of vegetation throughout the year. |
| Water bodies | Artificial water harvesting aquifers |
| Vegetation cover | Areas covered by vegetation, mainly *Acacia spp* trees with dense growth of trees that forms nearly closed canopies |
| Built-up | Comprises residential areas (IDPs camp, small villages, and/or rural settlements). |
| Wadi | Areas dominated by sand, including seasonal water streams. |

adequate number of samples for each LULC category. This method helped reduce spatial bias and enhance classification accuracy. To account for seasonal variability and long-term land cover changes, training data were sourced from multi-year imagery rather than a single time point. This approach improves model robustness by capturing variations in vegetation phenology and land use dynamics. To ensure a balanced and unbiased accuracy assessment, 50% of the training samples were used for classification, while the remaining 50% were reserved for validation. This strategy minimizes overfitting risks and provides a more reliable estimate of model generalization, preventing inflated accuracy results due to insufficient test data [36]. The second step in the image classification was image segmentation using OTB plugin in QGIS. This method converts pixels with similar characteristics into polygons. We made extensive trial-and-error experiments to find the optimal parameters for the image segmentation. In our case, we trained the data using TrainVectorClassifier with two different machine learning algorithms, Support Vector Machine (SVM) and Random Forest (RF) classifier. Those commonly used machine learning algorithms as specified in Ref. [37], were deemed to be the most suitable supervised classifiers because of their excellent classification performance.

### 2.6. Accuracy assessment

Accuracy assessment is a crucial step in the classification process, providing a quantitative evaluation of how effectively pixels are assigned to the correct land cover classes. In this study, an accuracy assessment was performed for LULC classifications in 2017, 2019, 2021, and 2023 to evaluate the performance of the classification algorithms in distinguishing various LULC categories. The reliability of the accuracy assessment depends on the availability of precise ground truth or reference data. To obtain reference data, high-resolution satellite imagery from Google Earth Pro was visually interpreted, supplemented by local knowledge of the study area from the first author. A stratified random sampling approach was applied, ensuring an equal number of samples for each land cover class. This sampling method was used for both training and validation, with classification accuracy evaluated using a confusion matrix, the most widely used approach for assessing image classification accuracy [38]. In addition to the confusion matrix, overall accuracy and the Kappa coefficient were computed. The Kappa coefficient, which ranges from negative values to 1, provides insight into classification agreement beyond random chance. A Kappa value of 1 indicates perfect agreement, 0 represents a classification no better than random assignment, and negative values suggest a classification worse than random. These accuracy metrics were used to assess the reliability and robustness of the classification results.

### 2.7. LULC change analysis

After the classification of satellite images, various analysis techniques were applied to determine the proportions of changes within the LULC categories in the study period 2017 to 2023. As a result, we used equations (2) and (3) to calculate the percentage and rate of change of a specific land cover over time. The analysis provides a sense of decline and growth in the specific classes, as well as the ability to comprehend LULC dynamics across the study period.

$$\% \text{ change} = \frac{\mathrm{X} - \mathrm{Y}}{Y} * 100 \qquad \text{Equation (2)}$$

$$\text{Rate of change}(ha\,/\,year) = \frac{\mathrm{X} - \mathrm{Y}}{Z} \qquad \text{Equation (3)}$$

where: X represents the area (ha) at time 2, Y represents the area (ha) at time 1, and Z is the Time interval between X and Y in years.

### 2.8. Implementation of SVM and RF classification algorithms

The SVM is a linear model for classification and regression that is mainly based on kernels, it was developed by Ref. [39]. SVMs have been utilized in this study as it widely used in remote sensing applications. SVM classifier aims to build a linear separation rule between objects in a dimensional space (hyperplane) using a mapping function derived from training samples. When two classes are nonlinearly separable, the approach uses the kernel method to realize projections of the feature space on higher dimensionality spaces, in which the separation of the classes is linear. In their simplest form, SVMs are linear binary classifiers that assign a certain test sample to a class using one of the two possible labels. Nonetheless, a multiclass classification is possible and is automatically executed by the algorithm.

The RF classifier, on the other hand, is an ensemble method that uses decision trees as classifiers. RF uses a large number of decision trees where each is feature-aggregated (bagging) by bootstrapping the training samples. The final output is determined by the majority vote of the trees. The RF is a powerful machine learning technique since it applies feature significant properties and averages several predictions [40,41]. During the construction, each tree is split at every internal node using the square root of the number of features (n). From the training data (n_features), which consists of the pixel values defined by the ROIs (regions of interest), the features are determined and chosen at random. Thus, a suitable size for the training dataset should be ensured. There is no predetermined size for this; it relies on the specific attributes of each dataset and the intended class number.

Experiences from Refs. [42,43] show that the default setting values of the OTB parameters for the training and classification process seem to provide optimal results. According to this, we used the default setting for both classification algorithms. For the RF, the maximum depth of the tree was set to 5, while the maximum number of trees was fixed to 100. The OOB error was set to 0.01. For the SVM we used a linear kernel-type with a model-type based on C value equal to 1. The study workflow is summarized in Fig. 2.

### 2.9. *Drought analysis*

Drought conditions in the study area were assessed using the Global 0.5° gridded SPEI database (SPEI-base), which calculates drought severity using precipitation and PET based on the FAO-56 Penman-Monteith method. The datasets accessed and downloaded from Google Earth Engine (GEE), were processed using R software to evaluate historical drought patterns in the study area. Three SPEI timescales were employed. SPEI-6 (Six-Month Scale) which captures short-to medium-term droughts affecting agriculture and pastoral systems; SPEI-9 (Nine-Month Scale) which reflects prolonged dry periods influencing soil moisture, groundwater recharge, and hydrological conditions and SPEI-12 (Twelve-Month Scale) which captures long-term drought trends and their cumulative impacts on ecosystems and socio-economic conditions.

The drought frequency was determined by counting events where SPEI values dropped below −1.0 (moderate drought threshold). Drought intensity was classified as: Extreme Drought: SPEI < −2.0, Severe Drought: −2.0 ≤ SPEI < −1.5, and Moderate Drought: −1.5 ≤ SPEI < −1.0 (Table 3). A drought event was considered to end once SPEI values returned to zero or transitioned into positive values. The analysis covered the period 2000–2023 to assess long-term drought dynamics. Table 3 shows the classification of drought intensity based on the SPEI index.

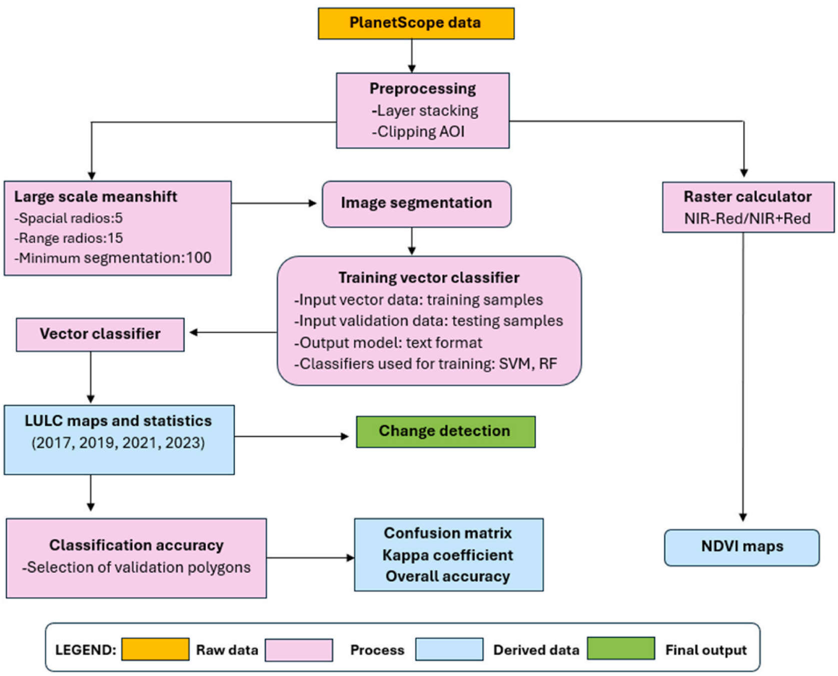


**Fig. 2.** Schematic diagram showing a summary of the study workflow.

**Table 3**
Classification of drought intensity based on the SPEI drought index.

| Drought category | Normal | Mild drought | Moderate drought | Severe drought | Extreme drought |
|---|---|---|---|---|---|
| **SPEI value** | < −0.5 | −0.5 to −1.0 | −1.0 to −1.5 | −1.5 to −2.0 | >−2.0 |

## 3. Results

### *3.1. Classification accuracy and LULC statistics*

The LULC classification achieved high accuracies, with overall accuracies ranging between 90% and 95% for the Support Vector Machine (SVM) algorithm and between 78% and 95% for Random Forest (RF) (Table 4). Six LULC classes were mapped and characterized for the years 2017, 2019, 2021, and 2023 (Fig. 3). In 2017, agricultural land was the predominant LULC class, covering 48.26% (11,792.95 ha) of the study area, followed by bareland at 46.82% (11,442.64 ha), Wadi at 2.76% (673.87 ha), built-up areas at 1.41% (344.95 ha), vegetation cover at 0.75% (182.76 ha), and water bodies at a minimal 0.001% (0.18 ha) (Table 5).

In 2019, agricultural land slightly decreased to 47.96% (11,721.09 ha), while bareland remained relatively stable at 46.85% (11,449.57 ha). The Wadi, built-up areas, vegetation cover, and water bodies occupied smaller portions at 2.80% (683.67 ha), 1.42% (338.14 ha), 0.96% (233.77 ha), and 0.005% (1.11 ha), respectively. By 2021, agricultural land expanded marginally to 48.02% (11,735.42 ha), with bareland decreasing to 45.93% (11,224.39 ha). The Wadi increased to 3.49% (853.23 ha), while built-up areas, vegetation cover, and water bodies occupied 1.48% (361.43 ha), 1.07% (261.51 ha), and 0.006% (1.37 ha), respectively. In 2023, agricultural land showed a significant increase to 54.61% (13,344.38 ha), while bareland decreased to 39.31% (9607.24 ha). Wadi covered 2.96% (723.94 ha), vegetation cover grew to 1.60% (391.09 ha), built-up areas slightly increased to 1.50% (367.36 ha), and water bodies expanded to 0.014% (3.34 ha).

Overall, the results indicate a clear trend of increasing agricultural land, vegetation cover, built-up areas, and water bodies, with a corresponding decrease in bareland over the study period.

### *3.2. Vegetation health condition*

Vegetation health was assessed using the Normalized Difference Vegetation Index (NDVI), a key spectral index in this study (Fig. 4). The NDVI values ranged from −0.17 to +0.67, where six distinct classes of vegetation health were identified based on these threshold values. The analysis revealed a significant increase in vegetation cover over the study period. This improvement is likely due to the overall rise in mean annual precipitation and the widespread adoption of agroforestry practices along with natural regeneration in the region. Agroforestry, which integrates trees, crops, pasture, and/or livestock for economic, social, and environmental benefits, has been widely applied in the study area. This practice helps reduce pressure on natural forests and contributes significantly to reforestation and forest rehabilitation efforts.

### *3.3. LULC changes and change rates*

Table 6 presents the overall area changes (ha), rate of area changes (ha/year) and the percentage of changes (%) from 2017 to 2023 in the study area. Agricultural land had the largest positive change and expanded by (1551.43 ha). This expansion corresponds to a 13.15% increase and an average annual growth rate of 258.57 ha/year. Bareland underwent the most reduction, shrinking by 1835.40 ha, or −16.06%, at an average rate of −305.90 ha/year. Water Bodies, despite being a minor class experienced a remarkable percentage increase (1755.55%) due to a small absolute gain of 3.16 ha, at an annual increased rate of 0.52 ha/year. Vegetation cover improved by 208.33 ha (+113.99%), with an annual increase of 34.72 ha/year. Built-up areas increased modestly by 22.41 ha (+6.49%), averaging 3.73 ha/year. The Wadi areas expanded by 50.07 ha (7.43%), with an annual increase of 8.34 ha/year.

Overall, the analysis indicates significant land transformation, particularly the shift from bareland to agricultural and vegetation areas.

**Table 4**
The accuracy of LULC cover maps of the study area (2017, 2019, 2021, and 2023).

| ML Algorithm | 2017 | | 2019 | | 2021 | | 2023 | |
|---|---|---|---|---|---|---|---|---|
| | Overall Accuracy in (%) | Kappa coefficient | Overall Accuracy in (%) | Kappa coefficient | Overall Accuracy in (%) | Kappa coefficient | Overall Accuracy in (%) | Kappa coefficient |
| Support vector machine (SVM) | 92.53 | 0.89 | 95.14 | 0.93 | 92.55 | 0.87 | 90.66 | 0.86 |
| Random Forest (RF) | 88.03 | 0.83 | 95.11 | 0.93 | 88.41 | 0.82 | 78.57 | 0.69 |

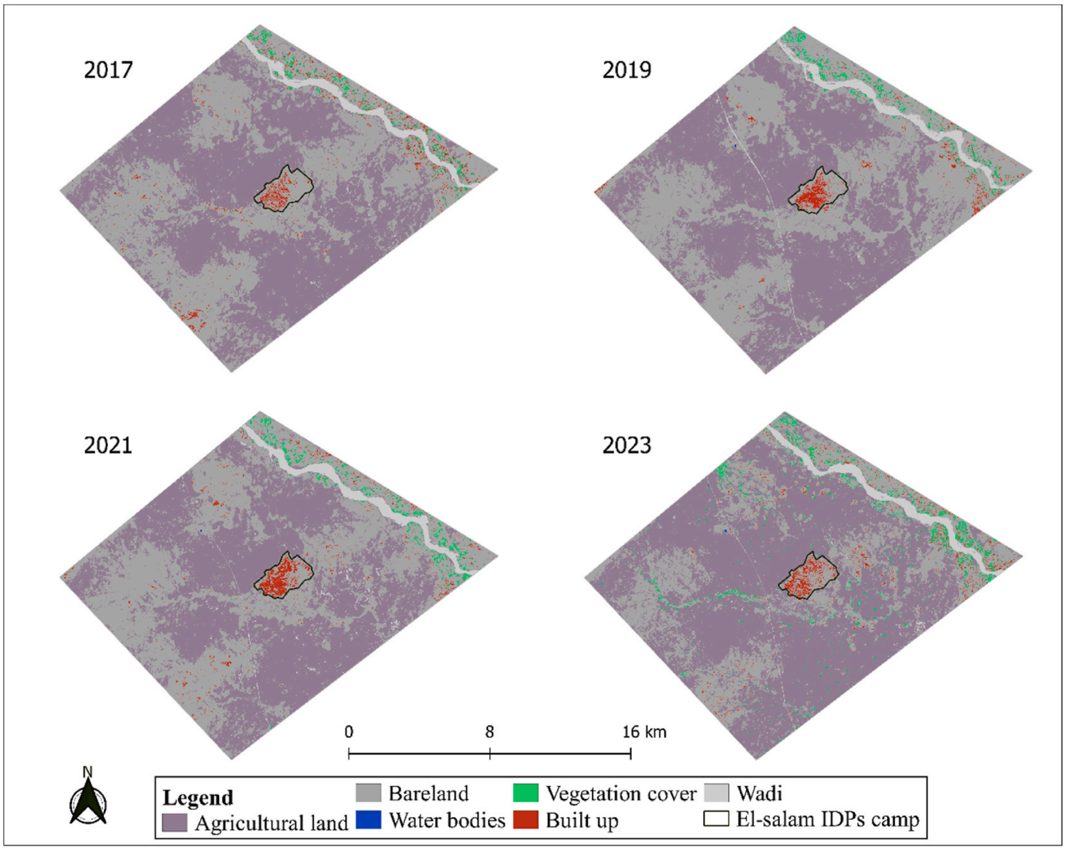


**Fig. 3.** Classified LULC Maps of the study area (2017, 2019, 2021 and 2023).

**Table 5**
LULC area statistics of the study region from 2017 to 2023.

| LULC classes | 2017 | | 2019 | | 2021 | | 2023 | |
|---|---|---|---|---|---|---|---|---|
| | Area (ha) | Area (%) | Area (ha) | Area (%) | Area (ha) | Area (%) | Area (ha) | Area (%) |
| **Agricultural land** | 11792.95 | 48.26 | 11721.09 | 47.96 | 11735.42 | 48.02 | 13344.38 | 54.61 |
| **Bareland** | 11442.64 | 46.82 | 11449.57 | 46.85 | 11224.39 | 45.93 | 9607.24 | 39.31 |
| **Water bodies** | 0.18 | 0.001 | 1.11 | 0.005 | 1.37 | 0.006 | 3.34 | 0.014 |
| **Vegetation cover** | 182.76 | 0.75 | 233.77 | 0.96 | 261.51 | 1.07 | 391.09 | 1.60 |
| **Built up** | 344.95 | 1.41 | 348.14 | 1.42 | 361.43 | 1.48 | 367.36 | 1.50 |
| **Wadi** | 673.87 | 2.76 | 683.67 | 2.80 | 853.23 | 3.49 | 723.94 | 2.96 |
| **Total** | 24437.35 | 100.00 | 24437.35 | 100.00 | 24437.35 | 100.00 | 24437.35 | 100.00 |

### *3.4. LULC change transition matrix*

During the initial phase of our study spanning from 2017 to 2019, the change matrix analysis indicated that about 83.77% (20472.36 ha) of the area remained unchanged, whereas 16.23% (3964.99 ha) underwent various changes, as shown in Table 7. The results of the changes showed about 1456.51 ha, 0.90 ha, 143.59 ha, 244.28 ha, and 68.02 ha of bareland converted to agricultural land, water bodies, vegetation cover, built up, and wadi, respectively. Additionally, about 1477.33 ha, 0.22 ha, 3.66 ha, 3.59 ha, and 65.10 ha of agricultural land were converted to bareland, water bodies, vegetation cover, built-up, and wadi, respectively.

In the second phase (2019 to 2021), 83.46% (20,389.69 ha) of the land remained unchanged while 16.54% (4047.66 ha) of land changed (Table 8). Bareland decreased significantly (−2071.59 ha), with most of it transitioning to agriculture (1487.16 ha) and vegetation cover (165.43 ha). Vegetation recovery was evident as 165.43 ha of bareland turned into vegetation cover, indicating reforestation or land restoration. A portion of agricultural land (4.26 ha) was converted to vegetation cover pointing towards the contribution of agroforestry to vegetation recovery.

During the third period of our study, 2021 to 2023, the results of the change matrix revealed that about 83% (20283.28 ha) of the area remained unchanged, whereas 17% (4154.07 ha) were changed, as shown in Table 9. The results of the change showed about

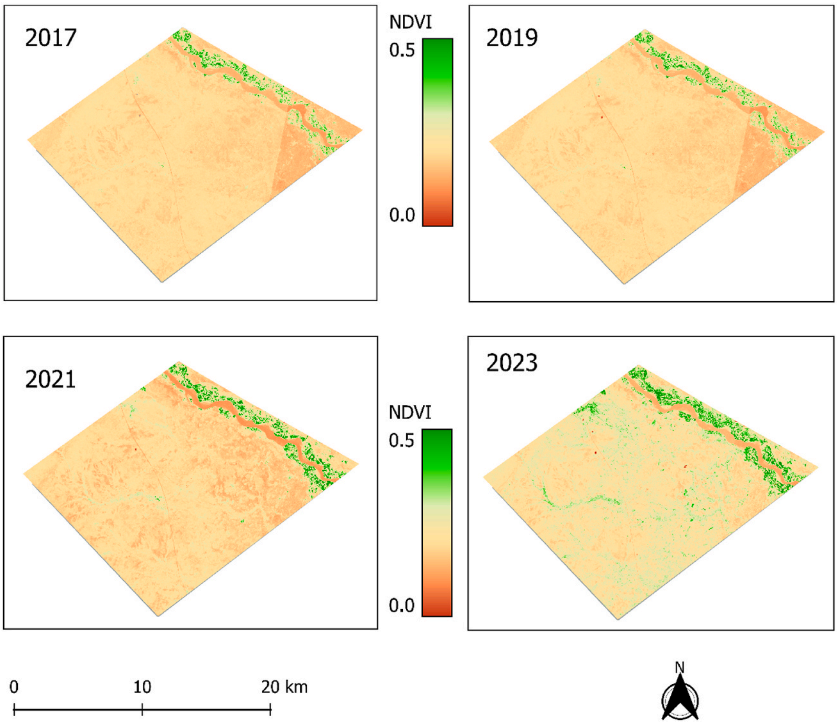


**Fig. 4.** NDVI maps of the study area (2017, 2019, 2021, and 2023).

**Table 6**
The overall area, percentage and rate of area changes in LULC classes from 2017 to 2024 in the study area.

| Period | Area changes | LULC classes | | | | | |
|---|---|---|---|---|---|---|---|
| | | Agricultural land | Bareland | Water bodies | Vegetation | Built up | Wadi |
| **2017–2023** | **(ha)** | 1551.43 | −1835.40 | 3.16 | 208.33 | 22.41 | 50.07 |
| | **(%)** | 13.15 | −16.06 | 1755.55 | 113.99 | 6.49 | 7.43 |
| | **ha/year** | 258.57 | −305.90 | 0.52 | 34.72 | 3.73 | 8.34 |

2291.11 ha, 1.12 ha, 251.98 ha, 192.23 ha and 26.07 ha of bareland converted to agricultural land, water bodies, vegetation cover, built up and wadi, respectively. Furthermore, about 777.51 ha, 0.22 ha, 21.69 ha, 2.25 ha and 41.79 ha of agricultural land were converted to bareland, water bodies, vegetation cover, built-up, and wadi, respectively.

Overall, the analysis reveals substantial land transformation, particularly the conversion of bareland into agricultural land, built-up areas, and vegetative cover. During the first period of our study (2017 to 2019), there was a notable reduction in bareland, which largely transitioned into agricultural land, built-up areas, and vegetation. Similarly, in the second period (2021 to 2023), bareland continued to decrease significantly, predominantly converting into agricultural land and vegetation cover.

### *3.5. Drought frequency and intensity analysis*

The SPEI time series analysis across 6-month, 9-month, and 12-month timescales are presented in Fig. 5. Prolonged drought conditions were identified between 2001 and 2011, contributing to severe vegetation degradation and environmental stress. In contrast, the period 2013–2023 exhibited reduced drought frequency and intensity, correlating with improved precipitation patterns and subsequent vegetation recovery. Drought intensity classification (Fig. 6) confirmed that mild drought was the most frequent category, followed by normal conditions. However, severe and extreme droughts were prevalent between 2001 and 2011, with intermittent wet periods in 2000, 2003, and 2008.

### *3.6. Rainfall and temperature trends analysis*

Fig. 7 illustrates a steady increase in annual rainfall in the study area over the study period, particularly from 2014 onwards. High inter-annual variability was observed from 2000 to 2013, followed by a more stable wet trend from 2014 to 2022. Temperature analysis (Fig. 8) revealed consistent warming patterns. The maximum temperature (~44°C) remained relatively stable with minor

**Table 7**
LULC change matrix (2017–2019).

| | | 2019 | | | | | | |
|---|---|---|---|---|---|---|---|---|
| | LULC Types | Agricultural land | Bareland | Water bodies | Vegetation cover | Built up | Wadi | Total |
| **2017** | Agricultural land | 10243.04 | 1477.33 | 0.22 | 3.66 | 3.59 | 65.10 | 11792.95 |
| | Bareland | 1456.51 | 9529.35 | 0.90 | 143.59 | 244.28 | 68.02 | 11442.64 |
| | Water bodies | 0.00 | 0.09 | 0.00 | 0.00 | 0.05 | 0.05 | 0.18 |
| | Vegetation cover | 3.42 | 99.66 | 0.00 | 66.63 | 8.58 | 4.49 | 182.76 |
| | Built up | 1.77 | 227.59 | 0.00 | 19.63 | 91.64 | 4.31 | 344.95 |
| | Wadi | 16.35 | 115.56 | 0.00 | 0.25 | 0.00 | 541.70 | 673.87 |
| | Total | 11721.09 | 11449.57 | 1.11 | 233.77 | 348.14 | 683.67 | 24437.35 |

**Table 8**
LULC change Matrix (2019–2021).

| | | 2021 | | | | | | |
|---|---|---|---|---|---|---|---|---|
| | LULC Types | Agricultural land | Bareland | Water bodies | Vegetation cover | Built up | Wadi | Total |
| **2019** | Agricultural land | 10189.10 | 1482.87 | 0.02 | 4.26 | 0.56 | 44.28 | 11721.09 |
| | Bareland | 1487.16 | 9377.98 | 0.07 | 165.43 | 222.64 | 196.29 | 11449.57 |
| | Water bodies | 0.00 | 0.11 | 1.01 | 0.00 | 0.00 | 0.00 | 1.11 |
| | Vegetation cover | 3.30 | 146.92 | 0.00 | 77.45 | 2.19 | 3.90 | 233.77 |
| | Built up | 1.28 | 195.59 | 0.26 | 14.32 | 136.04 | 0.65 | 348.14 |
| | Wadi | 54.59 | 20.93 | 0.00 | 0.04 | 0.00 | 608.11 | 683.67 |
| | Total | 11735.42 | 11224.39 | 1.37 | 261.51 | 361.43 | 853.23 | 24437.35 |

**Table 9**
LULC change matrix (2021–2023).

| | | 2023 | | | | | | |
|---|---|---|---|---|---|---|---|---|
| | LULC Types | Agricultural land | Bareland | Water bodies | Vegetation cover | Built up | Wadi | Total |
| 2021 | Agricultural land | 10891.97 | 777.51 | 0.22 | 21.69 | 2.25 | 41.79 | 11735.42 |
| | Bareland | 2291.11 | 8461.79 | 1.12 | 251.98 | 192.33 | 26.07 | 11224.39 |
| | Water bodies | 0.00 | 0.25 | 1.11 | 0.00 | 0.00 | 0.00 | 1.37 |
| | Vegetation cover | 2.10 | 129.13 | 0.00 | 115.01 | 11.90 | 3.36 | 261.51 |
| | Built up | 1.27 | 196.93 | 0.00 | 2.22 | 160.85 | 0.17 | 361.43 |
| | Wadi | 157.94 | 41.64 | 0.88 | 0.20 | 0.03 | 652.55 | 853.23 |
| | Total | 13344.38 | 9607.24 | 3.34 | 391.09 | 367.36 | 723.94 | 24437.35 |

fluctuations. The mean temperature (∼35°C) exhibited a slight warming trend. Minimum temperature (∼10°C) showed high inter-annual variability, with an overall warming trend.

## 4. Discussion

### *4.1. LULC changes*

This study utilized high-resolution multispectral PlanetScope imagery with 3-m spatial resolution to analyze LULC changes, particularly focusing on vegetation cover in the vicinity of the El-Salam IDPs camp. The results show a steady increase in built-up areas, suggesting ongoing development and a growing displaced population. Agricultural land expanded at an average rate of 3.09 ha/year, likely to meet the food demands of the growing IDPs population, aligning with the national adaptation strategy. Vegetation cover in the study area exhibited significant growth, largely attributed to reforestation initiatives, improved land management practices, natural regeneration, and increased precipitation.

### *4.2. Role of IDPs in vegetation recovery*

Studies have shown that IDPs, despite being displaced due to conflict, often engage in community-led land restoration efforts to rebuild their livelihoods and secure essential resources [16]. In Darfur, reforestation efforts were initiated in 2014 by the Forest National Corporation (FNC) in collaboration with other organizations such as the United Nations Environment Programme (UNEP), local NGOs and the IDP communities to implement tree-planting initiatives, sustainable agriculture programs, and agroforestry projects [45]. These activities have been critical in increasing vegetation cover, mitigating soil degradation, and enhancing ecological resilience in conflict-affected landscapes [46]. Additionally, research indicates that reforestation and sustainable land management practices in IDPs settlements often emerge as adaptive strategies to combat deforestation caused by high fuelwood demand [47]. Many IDPs in Darfur have integrated tree planting with the cultivation of drought-resistant crops, improving soil fertility and water retention, which has contributed to the observed vegetation regrowth [45]. Agroforestry integrates tree-based systems within agricultural landscapes, which in the long run contributes to an increase in the vegetation cover. Key agroforestry tree species introduced during these initiatives include *Acacia mellifera, Acacia senegal, Balanites aegyptiaca, Azadirachta indica, Khaya senegalensis, Faidherbia albida*, and various *Eucalyptus* species, promoting biodiversity and resilience in the local ecosystems. Furthermore, artificial water harvesting systems constructed in and around IDP camps have supported tree survival and increased green cover, even under semi-arid conditions [48]. These findings are consistent with those by Ref. [16], who observed sustainable vegetation growth in refugee areas in eastern Sudan, and [49] who emphasized IDPs' role in reforestation projects aimed at improving soil health.

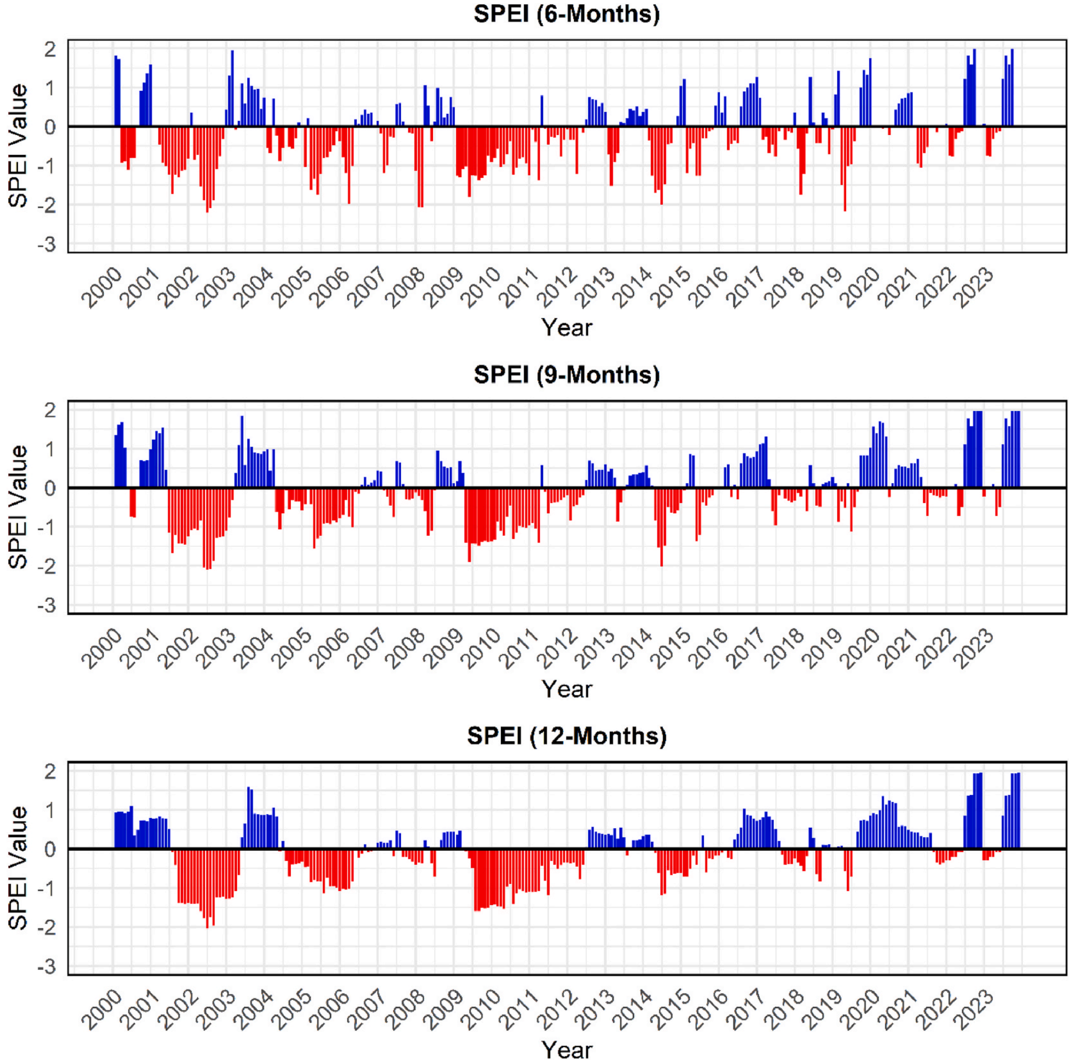


**Fig. 5.** SPEI time series analysis of the study area (2000–2023).

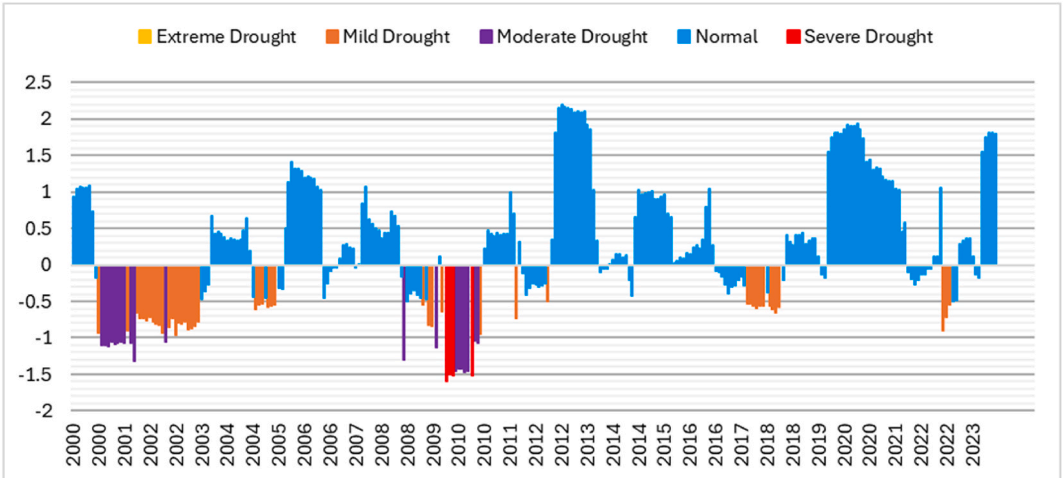


**Fig. 6.** Drought intensity analysis in the study area (2000–2023).

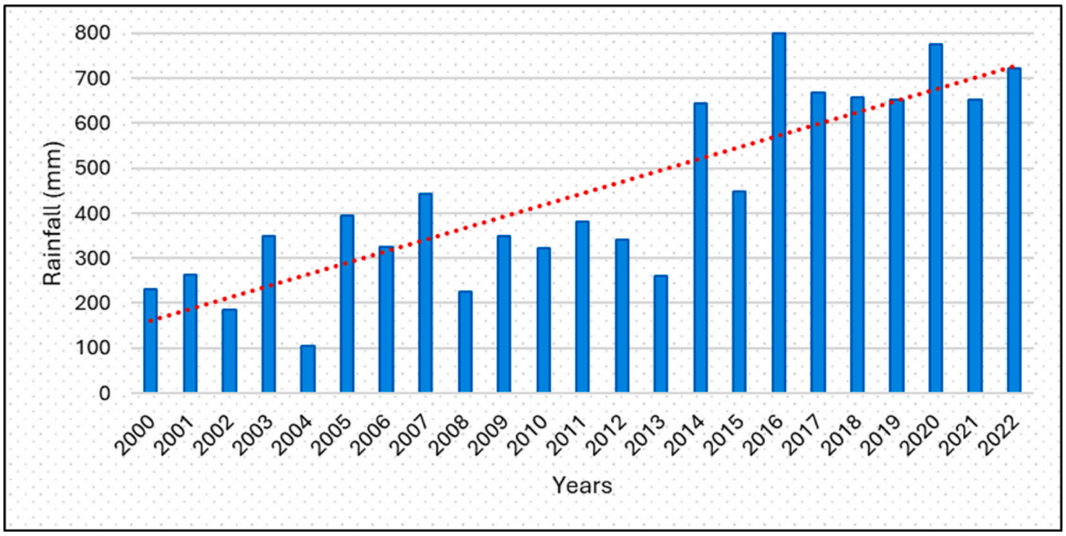


**Fig. 7.** Mean annual rainfall and temperature time series data of the study area from 2000 to 2022 [44].

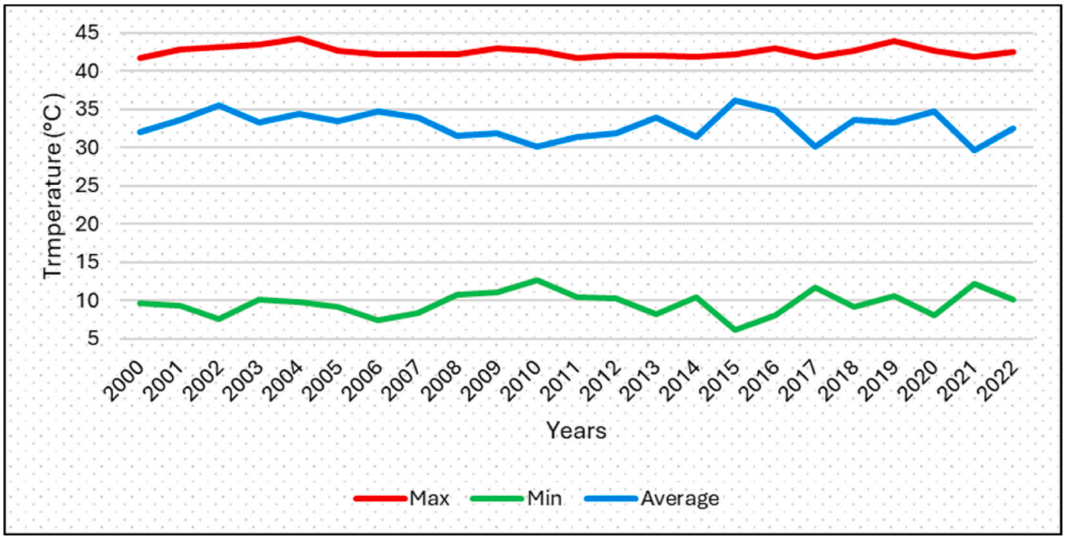


**Fig. 8.** Maximum, Mean, and Minimum annual temperature in the study area (2000–2022).

### *4.3. Climate variability, water management and vegetation recovery*

In the present study, a steady increase in average annual rainfall was recorded in the study area, particularly from 2014 onwards (Fig. 7). This increase in precipitation complemented the afforestation efforts by boosting the survival of the afforested seedlings and trees. Studies by other researchers like [28]. Have likewise demonstrated the link between vegetation dynamics and climatic factors, highlighting rainfall as a key driver of vegetation growth. Research by Ref. [50] in the Sudano-Sahelian region, which includes Sudan, found that long-term rainfall variability from 2001 to 2020 significantly contributed to increased vegetation greenness, with around half of the areas exhibiting greening attributed to changes in rainfall patterns. Similarly [51], noted that increased precipitation not only enhanced vegetation greening but also augmented regional water cycles, affecting runoff and water storage, which in turn promoted further vegetation recovery. These findings collectively underscore the critical role of both human interventions and climatic factors in driving positive vegetation changes in the region. Studies such as [52] Indicate that the region was predominantly characterized by extensive bareland with minimal vegetation cover, largely due to land degradation, deforestation, and prolonged drought. Additionally, these studies highlight a clear link between the increasing IDP camp population and the depletion of natural resources in the surrounding areas. The observed increase in vegetation cover after 2014 (Fig. 9) can therefore be attributed to reforestation initiatives, improved land management practices, and increased precipitation.

The marked increase in water bodies underscores enhanced water management practices, including the construction of artificial

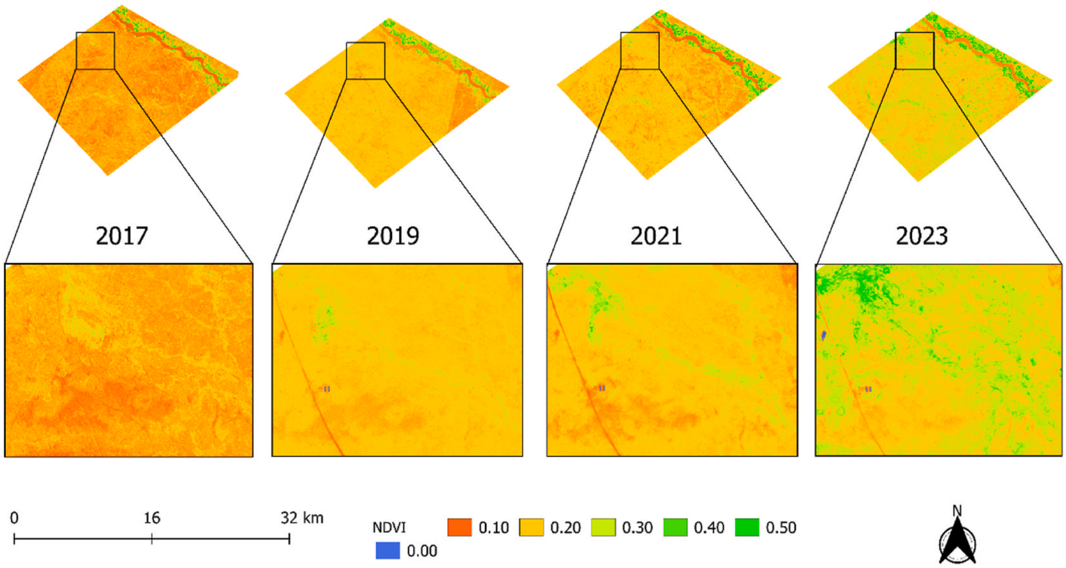


**Fig. 9.** NDVI maps highlighting the vegetation recovery trends in 2017, 2019, 2021, and 2023. A zoomed-in view of the northern part of the study area is presented to emphasize localized rehabilitation patterns.

water storage systems. This improved water availability likely supported agroforestry efforts, a trend also documented by Ref. [53], which noted that both natural and artificial water systems have played a critical role in environmental recovery in Darfur [54]. similarly emphasized the importance of water harvesting and small dams in sustaining agriculture and reforestation in conflict-affected areas, further validating these findings [55]. also demonstrated how water management practices, such as artificial aquifers and the cultivation of drought-tolerant crops, significantly increased vegetation cover in semi-arid regions of Ethiopia, which share similar climatic conditions with Darfur [56]. provided further support for the role of artificial water storage in boosting vegetation cover and supporting agroforestry, particularly in regions where rainfall is variable. A decrease in bareland was observed, likely due to its conversion to agricultural land. Wadis in arid and semi-arid regions are inherently dynamic, with their extent fluctuating due to rainfall variability, sediment deposition, and surface runoff patterns. Periods of increased precipitation have likely contributed to Wadi expansion through higher runoff and sediment transport. Conversely, reductions in Wadi extent may be attributed to sediment accumulation, vegetation encroachment, and land management practices such as agroforestry and reforestation, which stabilize riverbanks and regulate water flow. Furthermore, human interventions including water diversion for agriculture, soil conservation efforts, and infrastructure development may have altered Wadi morphology over time.

SPEI analysis confirmed that 2001–2012 was a prolonged drought period, significantly contributing to land degradation. However, a notable reduction in drought events post-2013, alongside increased rainfall, facilitated vegetation recovery. These findings align with broader Sahelian studies that emphasize precipitation as a primary driver of vegetation health. Additionally, research by Ref. [57] on long-term climate trends in Sudan provides a broader context for these environmental shifts. Our study further supports the role of SPEI as a more comprehensive drought index, capturing both precipitation and temperature influences, and highlights the importance of integrating multiple climatic indicators to assess vegetation dynamics effectively.

Overall, this study emphasizes the positive role of reforestation and rainfall in enhancing vegetation cover in conflict-affected regions like Darfur.

### *4.4. Ecological and economic implications of LULC changes*

The environmental implications of this research are multifaceted, revealing critical insights into ecological, economic, and social dynamics in the region. The positive changes in vegetation cover signal improved ecological balance, promoting biodiversity, healthier soils, and resilience against environmental degradation [58]. The increase in agricultural land and built-up areas suggests potential economic development, offering improved livelihoods, food security, and reduced dependency on external aid within the internally displaced community [59]. Climate resilience emerges as a key theme, with the study underscoring the role of rainfall in vegetation recovery, which can inform strategies to ensure sustainable land use despite climatic variability [28,60]. Effective resource management is emphasized, particularly in mitigating the environmental pressures exerted by IDP camps, such as through sustainable agricultural practices and alternative energy sources [16]. Policymakers can leverage these findings to craft strategies that promote reforestation, land management, and community engagement, driving sustainable development [21]. Vegetation regrowth can enhance soil structure, reduce erosion, increase organic matter content, and improve nutrient cycling. However, without direct assessments, the extent of these benefits remains uncertain. Restored vegetation can promote habitat connectivity and ecosystem stability, but further research is needed to evaluate species diversity, wildlife recovery, and overall biodiversity gains. Vegetation cover plays a crucial role in water infiltration, sediment retention, and hydrological regulation [61]. Future studies could assess how land cover changes influence water quality, particularly in arid regions.

The study also highlights the importance of community empowerment, as participatory approaches in reforestation have proven successful in enhancing vegetation cover. Long-term monitoring of land use changes and climate factors remains essential for adaptive management and sustained positive outcomes. Finally, addressing the environmental pressures from IDP camps through sustainable practices is critical for maintaining ecological balance.

### 4.5. Climate projections and vegetation sustainability

Future climate scenarios, as outlined in the Shared Socioeconomic Pathways (SSPs) and Representative Concentration Pathways (RCPs), provide valuable insights into potential climate trajectories and their implications for vegetation dynamics in arid regions such as Darfur. Under low-emission scenarios (SSP1-2.6, SSP2-4.5), projections indicate stable or slightly increasing precipitation patterns, which could further support and enhance vegetation recovery. However, under high-emission scenarios (SSP3-7.0, SSP5-8.5), rising temperatures, increased evapotranspiration, and shifting precipitation regimes could counteract recent vegetation gains, accelerate land degradation, and intensify resource competition. More frequent and severe droughts, as projected for arid and semi-arid regions, pose a significant risk to the long-term sustainability of current recovery trends. Sustainable reforestation and land restoration efforts require long-term political stability, governance support, and community engagement. However, given Darfur's history of conflict and displacement, political instability may disrupt conservation programs, hinder restoration efforts, and increase pressure on recovering ecosystems due to unsustainable land use practices. To ensure long-term vegetation sustainability, future studies should explore adaptive land-use planning, the use of drought-resistant tree species, and the role of local governance in conservation strategies. An integrated approach that combines climate adaptation measures, community-led afforestation programs, and sustainable land management policies will be essential in mitigating climate and political uncertainties.

### 4.6. Impact of ongoing conflict on reforestation and land use sustainability

Conflict disrupts reforestation initiatives by restricting land access, reducing government and NGO support, and displacing local communities who would otherwise participate in afforestation and conservation activities [62]. Insecurity often compels communities to exploit vegetation for fuelwood and livelihood needs, undermining long-term restoration efforts. Additionally, the destruction of infrastructure and governance systems during conflicts hinders the effective implementation and monitoring of reforestation programs.

In terms of agricultural land use, conflict-driven displacement frequently leads to abandoned farmland, which can result in either land degradation or, in some cases, passive reforestation [63]. However, the return of displaced populations can intensify land competition, deforestation, and changes in agricultural practices, as people reclaim farmland under unstable conditions. Weakened governance structures may also lead to unregulated land expansion, exacerbating environmental degradation and resource conflicts [64]. To ensure the long-term sustainability of both reforestation and agricultural land use, an integrated approach that considers both environmental and socio-political dynamics is essential. Future research should explore conflict-sensitive conservation strategies, such as engaging local communities in peace-building efforts through sustainable land management and strengthening governance mechanisms that promote both reforestation and equitable land access.

## 5. Conclusions

This study identified the major LULC classes in the Darfur region of Sudan, including agricultural land, built-up areas, vegetation cover, bareland, water bodies, and Wadi, achieving an overall classification accuracy of 90.66% to 95.14%. The key findings reveal a significant increase in agricultural land, built-up areas, and vegetation cover, alongside a decrease in bareland. The positive vegetation changes, particularly around the El-Salam IDP camps, are largely attributed to reforestation initiatives, improved land management, natural regeneration, and increased rainfall. The expansion of agricultural and built-up areas suggests economic growth, improved livelihoods, and a shift towards greater self-sufficiency within the IDP community. The study highlights the critical influence of climatic factors, especially rainfall, on vegetation recovery and emphasizes the need for adaptive strategies to enhance climate resilience. Moreover, the success of participatory approaches to afforestation and agroforestry practices underscores the vital role of community engagement in sustainable land management. These insights provide valuable guidance for policymakers and stakeholders aiming to promote ecological balance, resource management, and sustainable development in conflict-affected regions.

The use of remote sensing for LULC classification, drought indices (SPEI), and vegetation recovery assessment is a well-established method that can be applied to other arid and semi-arid regions experiencing land degradation, resource competition, and environmental recovery efforts. Our integrated approach combining climate analysis, human-induced factors, and post-conflict reforestation efforts can serve as a model for studying environmental changes in fragile and conflict-prone settings. However, we also acknowledge that local ecological conditions, governance structures, and sociopolitical dynamics influence vegetation recovery and LULC patterns differently across regions. To improve the generalizability of our findings, future research could apply similar methodologies to other conflict-affected areas while incorporating region-specific variables such as land tenure policies, displacement patterns, and conflict intensity. Additionally, we recognize the need for on-the-ground socioeconomic assessments to complement remote sensing analysis. As a recommendation for future research, we propose conducting detailed socioeconomic surveys and key informant interviews when conditions allow, to further investigate the underlying socio-economic factors contributing to LULC changes. This will provide a more holistic understanding of human-environment interactions in the study area.

## CRediT authorship contribution statement

**Abdalrahman Ahmed:** Writing – original draft, Methodology, Formal analysis, Conceptualization, Visualization, Writing – review & editing. **Brian Rotich:** Writing – review & editing, Writing – original draft, Visualization, Conceptualization. **Harison Kiplagat Kipkulei:** Writing – review & editing, Visualization, Methodology. **Kornel Czimber:** Supervision, Funding acquisition, Visualization, Writing – review & editing.

## Ethical statement

The authors of this study affirm that the research was carried out following ethical guidelines and regulations.

## Funding

This research received funds from "the project TKP2021-NVA-13, which was implemented with the support provided by the Ministry of Culture and Innovation of Hungary from the National Research, Development and Innovation Fund, financed under the TKP2021-NVA funding scheme."

## Declaration of competing interest

The authors declare that they have no known competing financial interests or personal relationships that could have appeared to influence the work reported in this paper.

## Acknowledgements

Much gratitude goes to the Sudanese Ministry of Higher Education and Scientific Research and the University of Gezira for their academic support, as well as the Tempus Public Foundation and the University of Sopron for providing a PhD scholarship to the first author. Gratitude also goes to the PlanetScope team for providing the Satellite data. PlanetScope data were provided by Planet Labs, within their education and research program.

## Data availability

Data will be made available on request. For requesting data, please write to the corresponding author.

## References

[1] E. Negash, E. Birhane, A. Gebrekirstos, M.A. Gebremedhin, S. Annys, M.M. Rannestad, D.H. Berhe, A. Sisay, T. Alemayehu, T. Berhane, B.M. Gebru, N. Solomon, J. Nyssen, Remote sensing reveals how armed conflict regressed woody vegetation cover and ecosystem restoration efforts in Tigray (Ethiopia), Sci of Rem Sens 8 (2023), https://doi.org/10.1016/j.srs.2023.100108.

[2] R. Reuveny, A.S. Mihalache-O'Keef, Q. Li, The effect of warfare on the environment, J. Peace Res. 47 (2010) 749–761, https://doi.org/10.1177/0022343310382069.

[3] P.R. Chowdhury, H. Medhi, K.G. Bhattacharyya, C.M. Hussain, Severe deterioration in food-energy-ecosystem nexus due to ongoing Russia-Ukraine war: a critical review, Sci. Total Environ. 902 (2023), https://doi.org/10.1016/j.scitotenv.2023.166131.

[4] L. Yasukawa, The impacts of internal displacement on local communities: examples from Ethiopia and Somalia, Refug. Surv. Q. 39 (2020) 544–551, https://doi.org/10.1093/RSQ/HDAA034.

[5] World Bank, World bank 2010, The impact of refugees on neighboring countries: a development challenge - google search. https://www.google.com/search?q=World+bank+2010.+The+impact+of+refugees+on+Neighboring+countries/3A+A+development+challenge&rlz=1C1GCEA_enHU1096HU1096&oq=World+bank+2010.+The+impact+of+refugees+on+Neighboring+countries/3A+A+development+challenge&gs_lcrp=E, 2010. (Accessed 15 May 2025).

[6] UNDP, Turning the tide on internal displacement: a megoldások fejlesztési megközelítése. https://data.undp.org/fr/insights/impact-displacement-idps, 2022. (Accessed 15 September 2024).

[7] M.H. Füssel, An Updated Assessment of the Risks from Climate Change Based on Research Published Since the IPCC Fourth Assessment Report, vol. 97, Springer, 2009, pp. 469–482, https://doi.org/10.1007/s10584-009-9648-5.

[8] J.S. Kikstra, Z.R.J. Nicholls, C.J. Smith, J. Lewis, R.D. Lamboll, E. Byers, M. Sandstad, M. Meinshausen, M.J. Gidden, J. Rogelj, E. Kriegler, G.P. Peters, J. S. Fuglestvedt, R.B. Skeie, B.H. Samset, L. Wienpahl, D.P. Van Vuuren, K.I. Van Der Wijst, A. Al Khourdajie, P.M. Forster, A. Reisinger, R. Schaeffer, K. Riahi, The IPCC sixth assessment report WGIII climate assessment of mitigation pathways: from emissions to global temperatures, Geosci. Model Dev. 15 (2022) 9075–9109, https://doi.org/10.5194/GMD-15-9075-2022.

[9] E. Gamreldin, M. Hamadalnel, E. Gamreldin, M. Hamadalnel, Spatial and temporal analysis of maximum and minimum temperature trends in Northern Sudan during (1990-2019), J. Geosci. Environ. Protect. 12 (2024) 266–288, https://doi.org/10.4236/GEP.2024.125015.

[10] Kotir, Climate Change and Variability in Sub-saharan Africa: a Review of Current and Future Trends and Impacts on Agriculture and Food Security, Springerjh KotirEnvironment, Development and Sustainability, vol. 13, Springer, 2011, pp. 587–605, https://doi.org/10.1007/s10668-010-9278-0, 2011.

[11] M.A.A. Osman, J.O. Onono, L.A. Olaka, M.M. Elhag, E.M. Abdel-Rahman, Climate variability and change affect crops yield under rainfed conditions: a case study in gedaref state, Sudan, Agronomy 11 (2021) 1680, https://doi.org/10.3390/AGRONOMY11091680, 11 (2021) 1680.

[12] M. Yvonne, G. Ouma, D. Olago, M.O.- Geography, Trends in climate variables (temperature and rainfall) and local perceptions of climate change in Lamu, Kenya, ges.Rgo.RuM Yvonne, G Ouma, D Olago, M OpondoGeography, undefined Environment, undefined 2020, Environ. Sustain. 13 (2020) 102–109, https://doi.org/10.24057/2071-9388-2020-24, 2020•ges.Rgo.Ru.

[13] M. Hamadalnel, Z. Zhu, R. Lu, M. Almazroui, S. Shahid, Evaluating the aptitude of global climate models from CMIP5 and CMIP6 in capturing the historical observations of monsoon rainfall over Sudan from 1946 to 2005, Int. J. Climatol. 42 (2022) 2717–2738, https://doi.org/10.1002/JOC.7387.

[14] M. Elhag, S. Walker, Impact of climate variability on vegetative cover in the Butana area of Sudan, Afr. J. Ecol. 47 (2009) 11–16, https://doi.org/10.1111/J.1365-2028.2008.01044.X.

[15] V. Nzabarinda, A. Bao, W. Xu, S. Uwamahoro, L. Jiang, Y. Duan, L. Nahayo, T. Yu, T. Wang, G. Long, Assessment and evaluation of the response of vegetation dynamics to climate variability in Africa, Sustainability 13 (2021) 1234, https://doi.org/10.3390/SU13031234, 13 (2021) 1234.

[16] S. Omer, M. Abdoun, Incentives for reforestation and forest's plantations option. Under the National Strategy of Redd+Program in Sudan, 2020.

[17] S. Jaspars, M. Buchanan-smith, Darfuri Migration from Sudan to Europe: from Displacement to Despair, 2018, pp. 1–144. https://www.odi.org/sites/odi.org.uk/files/resource-documents/12385.pdf.

[18] E. Gonzalez-Cueva, Saviors and survivors: darfur, politics and the War on terror, mahmood mamdani, Int. J. Transit. Justice 3 (2009) 465–470, https://doi.org/10.1093/IJTJ/IJP012.

[19] A. Gafaar, Forest plantations and woodlots in Sudan, African Forest Forum 1 (15) (2011). https://afforum.org/publication/forest-plantations-and-woodlots-in-sudan-vol-1-15/. (Accessed 15 May 2025).

[20] B. Bromwich, Power, contested institutions and land: repoliticising analysis of natural resources and conflict in Darfur, J Eastern African Studies 12 (2018) 1–21, https://doi.org/10.1080/17531055.2017.1403782.

[21] NAP, Republic of Sudan Ministry of Environment, Natural Resources and Physical Development Higher Council for Environment and Natural Resources (HCENR) National Biodiversity Strategy and Action Plan 2015-2020, 2015.

[22] Y. Elnour Yagoub, Z. Li, O. Said Musa, F. Wang, M. Naveed Anjum, Z. Bo, J. Ding-min, Detection of drought pattern in Sudan using standardized precipitation-evapotranspiration index (SPEI), Tgs.Ac.Cn. http://www.tgs.ac.cn/public/upfiles/file/20191127/1574843779579939.pdf, 2017. (Accessed 25 February 2025).

[23] N. Diffenbaugh, D. Swain, D.T.-P. of the National, Anthropogenic warming has increased drought risk in California, undefined 2015, Pnas.OrgNS Diffenbaugh, DL Swain, D ToumaProceedings of the National Academy of Sciences 112 (2015) 3931–3936, https://doi.org/10.1073/pnas.1422385112, 2015•pnas.Org.

[24] A. Ahmadalipour, H. Moradkhani, M.C. Demirel, A comparative assessment of projected meteorological and hydrological droughts: elucidating the role of temperature, J. Hydrol. 553 (2017) 785–797, https://doi.org/10.1016/J.JHYDROL.2017.08.047.

[25] W.O. Library, J.H. Stagge, L.M. Tallaksen, L. Gudmundsson, A.F. Van Loon, K. Stahl, Candidate distributions for climatological drought indices (SPI and SPEI), Wiley Online LibraryJH Stagge, LM Tallaksen, L Gudmundsson, AF Van Loon, K StahlInternational Journal of Climatology 35 (2015) 4027–4040, https://doi.org/10.1002/joc.4267, 2015•Wiley Online Library.

[26] M. Gašparović, M. Zrinjski, M. Gudelj, Automatic cost-effective method for land cover classification (ALCC), Comput. Environ. Urban Syst. 76 (2019) 1–10, https://doi.org/10.1016/J.COMPENVURBSYS.2019.03.001.

[27] T. Kavzoglu, S.R. Sensing, Performance analysis of maximum likelihood and artificial neural network classifiers for training sets with mixed pixels, Taylor & FrancisT Kavzoglu, S ReisGIScience & Rem Sens 45 (2008) 330–342, https://doi.org/10.2747/1548-1603.45.3.330, 2008•Taylor & Francis.

[28] Y.E. Yagoub, Z. Li, O.S. Musa, M.N. Anjum, F. Wang, C. Xu, Z. Bo, Investigation of vegetation cover change in Sudan by using Modis data, J. Geogr. Inf. Syst. 9 (2017) 279–292, https://doi.org/10.4236/jgis.2017.93017.

[29] T. Blaschke, Object based image analysis for remote sensing, ISPRS J. Photogrammetry Rem Sens. 65 (2010) 2–16, https://doi.org/10.1016/J.ISPRSJPRS.2009.06.004.

[30] A. Ahmed, B. Rotich, K. Czimber, Assessment of the environmental impacts of conflict-driven internally displaced persons: a sentinel-2 satellite based analysis of land use/cover changes in the Kas locality, Darfur, Sudan, PLoS One 19 (2024), https://doi.org/10.1371/journal.pone.0304034.

[31] A.A. Salih, M.B. Hussein, O. Bashir, Assessment the Food Security Situation of IDP ' S at Nyala Adjacent Camps, vol. 2, 2017, pp. 1–10, https://doi.org/10.13140/RG.2.2.21867.69926.

[32] J. Xue, X. Zhang, S. Chen, B. Hu, N. Wang, Z. Shi, Quantifying the agreement and accuracy characteristics of four satellite-based LULC products for cropland classification in China, J. Integr. Agric. 23 (2024) 283–297, https://doi.org/10.1016/J.JIA.2023.06.005.

[33] D. Ming, J. Li, J. Wang, M. Zhang, Scale parameter selection by spatial statistics for GeOBIA: using mean-shift based multi-scale segmentation as an example, ISPRS J. Photogrammetry Remote Sens. 106 (2015) 28–41, https://doi.org/10.1016/j.isprsjprs.2015.04.010.

[34] L. Zheng, J. Zhang, Q. Wang, Mean-shift-based color segmentation of images containing green vegetation, Comput. Electron. Agric. 65 (2009) 93–98, https://doi.org/10.1016/J.COMPAG.2008.08.002.

[35] R. Congalton, K. Green, Assessing the Accuracy of Remotely Sensed Data Principles and Practices, Third Edition, 2009.

[36] D. Yadav, K. Kapoor, A.K. Yadav, M. Kumar, A. Jain, J. Morato, Satellite image classification using deep learning approach, Earth Sci. Inform. 17 (2024) 2495–2508, https://doi.org/10.1007/S12145-024-01301-X/TABLES/5.

[37] H. Costa, G.M. Foody, D.S. Boyd, Supervised methods of image segmentation accuracy assessment in land cover mapping, Remote Sens. Environ. 205 (2018) 338–351, https://doi.org/10.1016/j.rse.2017.11.024.

[38] L. Plourde, R.G. Congalton, Sampling method and sample placement: how do they affect the accuracy of remotely sensed maps? Photogramm. Eng. Rem. Sens. 69 (2003) 289–297, https://doi.org/10.14358/PERS.69.3.289.

[39] C. Cortes, V. Vapnik, L. Saitta, Support-Vector Networks Editor, Kluwer Academic Publishers, 1995.

[40] V. Sudhakar, C. Venkata Sudhakar, G.U. Reddy, Limestone mining area mapping and assessment at the cement industrial area using spectral index and machine learning algorithms. https://doi.org/10.21203/rs.3.rs-2291023/v1, 2022.

[41] R.A. Rubo, C. de Carvalho Carneiro, M.F. Michelon, R. dos S. Gioria, Digital petrography: mineralogy and porosity identification using machine learning algorithms in petrographic thin section images, J. Pet. Sci. Eng. 183 (2019), https://doi.org/10.1016/j.petrol.2019.106382.

[42] M. Immitzer, F. Vuolo, C. Atzberger, First experience with Sentinel-2 data for crop and tree species classifications in central Europe, Remote Sens. 8 (2016), https://doi.org/10.3390/rs8030166.

[43] B.H. Trisasongko, D.R. Panuju, D.J. Paull, X. Jia, A.L. Griffin, Comparing six pixel-wise classifiers for tropical rural land cover mapping using four forms of fully polarimetric sar data, Int. J. Rem. Sens. 38 (2017) 3274–3293, https://doi.org/10.1080/01431161.2017.1292072.

[44] NASA, Power data acess. https://power.larc.nasa.gov/data-access-viewer/, 2023.

[45] FAO, REPUBLIC OF SUDAN IMPLEMENTATION OF NATIONAL FOREST MONITORING SYSTEM ACTION PLAN, 2021.

[46] E.B. Barbier, J.P. Hochard, Land degradation and poverty, Nat. Sustain. 11 (1) (2018) 623–631, https://doi.org/10.1038/s41893-018-0155-4, 2018 1.

[47] M. Funder, S. Marie Cold-Ravnkilde, I. Peters Ginsborg, Addressing climate change and conflict in development cooperation experiences from natural resource management. www.diis.dk, 2012. (Accessed 13 March 2025).

[48] D. Wen, X. Huang, F. Bovolo, J. Li, X. Ke, A. Zhang, J.A. Benediktsson, Change detection from very-high-spatial-resolution optical remote sensing images: methods, applications, and future directions, IEEE Geosci. Remote Sens. Mag. 9 (2021) 68–101, https://doi.org/10.1109/MGRS.2021.3063465.

[49] O. Kranz, A. Sachs, S. Lang, Assessment of environmental changes induced by internally displaced person (IDP) camps in the darfur region, Sudan, based on multitemporal MODIS data, Int. J. Rem. Sens. 36 (2015) 190–210, https://doi.org/10.1080/01431161.2014.999386.

[50] Y. Zeng, L. Jia, M. Menenti, M. Jiang, B.A. Barnieh, A. Bennour, Y. Lv, Changes in vegetation greenness related to climatic and non-climatic factors in the Sudano-Sahelian region, Reg. Environ. Change 23 (2023), https://doi.org/10.1007/s10113-023-02084-5.

[51] Z. Xu, H. Sun, T. Zhang, H. Xu, D. Wu, J.H. Gao, The high spatial resolution Drought response index (HiDRI): an integrated framework for monitoring vegetation drought with remote sensing, deep learning, and spatiotemporal fusion, Remote Sens. Environ. 312 (2024) 114324, https://doi.org/10.1016/J.RSE.2024.114324.

[52] K. Spröhnle, O. Kranz, E. Schoepfer, M. Moeller, S. Voigt, Earth observation-based multi-scale impact assessment of internally displaced person (IDP) camps on wood resources in Zalingei, Darfur, Geocarto Int. 31 (2016) 575–595, https://doi.org/10.1080/10106049.2015.1062053.

[53] UNEP, Rebuilding relationships over natural resources in Darfur. https://www.unep.org/news-and-stories/story/rebuilding-relationships-over-natural-resources-darfur, 2021. (Accessed 16 September 2024).

[54] FAO, Water management in fragile systems: building resilience to shocks and protracted crises in the Middle East and North Africa, water management in fragile systems: building resilience to shocks and protracted crises in the Middle East and North Africa. https://doi.org/10.1596/978-92-5-130614-7, 2018.

[55] J. Nyssen, J. Poesen, S. Lanckriet, M. Jacob, J. Moeyersons, M. Haile, N. Haregeweyn, R.N. Munro, K. Descheemaeker, E. Adgo, A. Frankl, J. Deckers, Land degradation in the Ethiopian Highlands, in: World Geomorphological Landscapes, Springer, 2015, pp. 369–385, https://doi.org/10.1007/978-94-017-8026-1_21.

[56] E.O. Ananga, R. Naiga, S.G. Agong', A.J. Njoh, H.P. Vickers, Examining the contribution of community participation in water resource production and management: perspectives from developing countries, SN Soc. Sci. 1 (2021), https://doi.org/10.1007/s43545-020-00050-0.

[57] C. Funk, G. Eilerts, J. Rowland, M. Marshall, Famine Early Warning Systems Network-Informing Climate Change Adaptation Series A Climate Trend Analysis of Sudan, 2011.

[58] R. Schimmer, Tracking the Genocide in Darfur : Population Displacement as Recorded by Remote Sensing, 2007.

[59] A. Eshitera, Assessing agricultural land carrying capacity for sustainable livelihoods and resettlement of internally displaced persons in South Darfur. http://essay.utwente.nl/93991/, 2013. (Accessed 15 May 2025).

[60] A. Ahmed, B. Rotich, K. Czimber, Climate change as a double-edged sword: exploring the potential of environmental recovery to foster stability in Darfur, Sudan, Climate 13 (2025) 63, https://doi.org/10.3390/CLI13030063, 13 (2025) 63.

[61] R. Teague, U. Kreuter, Managing grazing to restore soil health, ecosystem function, and ecosystem services, Front. Sustain. Food Syst. 4 (2020) 534187, https://doi.org/10.3389/FSUFS.2020.534187/BIBTEX.

[62] M. Gabay, M. Alam, Community forestry and its mitigation potential in the Anthropocene: the importance of land tenure governance and the threat of privatization, for, Policy Econ 79 (2017) 26–35, https://doi.org/10.1016/J.FORPOL.2017.01.011.

[63] L. de Jong, S. De Bruin, J. Knoop, J. van Vliet, Understanding land-use change conflict: a systematic review of case studies, J. Land Use Sci. 16 (2021) 223–239, https://doi.org/10.1080/1747423X.2021.1933226.

[64] S.B. Wassie, Natural resource degradation tendencies in Ethiopia: a review, Environ. Syst. Res. 9 (2020) 1–29, https://doi.org/10.1186/S40068-020-00194-1, 2020 9:1.